Convolutional Neural Networks with Transformed Input based on Robust Tensor Network Decomposition

Jenn-Bing Ong, Wee-Keong Ng
Nanyang Technological University
ongj0063, awkng@e.ntu.edu.sg

C.-C. Jay Kuo
University of Southern California
cckuo@sipi.usc.edu

Abstract

Tensor network decomposition, originated from quantum physics to model entangled many-particle quantum systems, turns out to be a promising mathematical technique to efficiently represent and process big data in parsimonious manner. In this study, we show that tensor networks can systematically partition structured data, e.g. color images, for distributed storage and communication in privacy-preserving manner. Leveraging the sea of big data and metadata privacy, empirical results show that neighboring subtensors with implicit information stored in tensor network formats cannot be identified for data reconstruction. This technique complements the existing encryption and randomization techniques which store explicit data representation at one place and highly susceptible to adversarial attacks such as side-channel attacks and de-anonymization. Furthermore, we propose a theory for adversarial examples that mislead convolutional neural networks to misclassification using subspace analysis based on singular value decomposition (SVD). The theory is extended to analyze higher-order tensors using tensor-train SVD (TT-SVD); it helps to explain the level of susceptibility of different datasets to adversarial attacks, the structural similarity of different adversarial attacks including global and localized attacks, and the efficacy of different adversarial defenses based on input transformation. An efficient and adaptive algorithm based on robust TT-SVD is then developed to detect strong and static adversarial attacks.
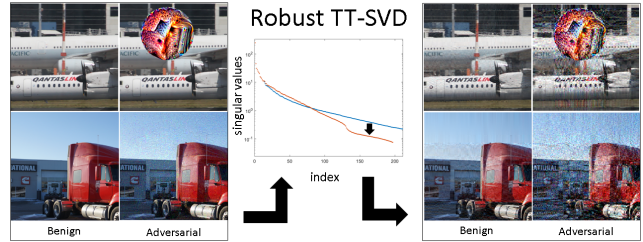
Figure 1. Global and localized adversarial examples, as diverse as their form can take, share similar structural properties in increasing the image roughness. This is because the sensitivity of subspace approximation by convolutional neural networks (CNNs) is controlled by the decay rate of singular values of the input image. The larger the decay rate, the smoother is the image input, and the more robust is the approximation. Our proposed robust TT-SVD algorithm linearly combines the singular values and vectors that fall within a (prescribed) bin to examine the robustness.

1. Introduction

Tensor computing recently emerges as a promising mathematical technique for big data processing and analytics [14, 16]. Big data serves as the fuel in driving deep learning models that create tremendous value for various applications, ranging from science, business, to government. Deep learning automates the process of feature extraction and exploits their compositionality to construct high-level features that achieve human-level performance in many designated tasks such as classification and prediction [44]. The tradeoff, however, involves storage and processing of large amount of (labeled) data and models with millions to billions of parameters. The data explosion growth is expected to outpace the development of storage and processing technology, therefore domain-specific hardware acceleration and algorithmic codesign all aim to improve throughput and energy-efficiency without compromising model performance and hardware costs to cater for widespread deployment of deep learning models [65]. Sharing of personal and confidential data across organizations demand cutting-edge privacy-preserving technology. Current privacy-preserving technologies such as encryption and randomization techniques share a common drawback that any security breaches such as leakage of decryption key or the data content during the storage, communication, or computation phases expose the individual records that contain explicit information. Therefore, it is timely and essential to explore new data structures which provide not only efficient and distributed storage and computation, but also privacy

1

preservation such that data leakage provides the adversary partial (implicit or latent) information of individual records and reconstruction is difficult without knowledge of the data structure.

Deep learning models, despite their impressive performance, are highly susceptible to adversarial attacks that attempt to perturb the inputs in subtle manner (imperceptible or quasi-imperceptible) to achieve the adversary's motives such as targeted or untargeted misclassifications. This has serious implications especially because these models are increasingly being deployed for mission-critical and safety-critical applications such as autonomous vehicles and robotics. Existing theories on adversarial examples such as models' linearity and non-linearity hypotheses, dimensional analyses, etc. do not generalize to different adversarial attacks, these theories typically stem from local empirical observations and do not fully align with each other [4]. In this paper, we conduct both theoretical and experimental studies using tensor networks as data structure for the input data of convolutional neural networks (CNNs) and analyze their robustness to adversarial attacks. Our contributions include:

- Propose to use tensor network representations for distributed storage of input data for machine learning models. In particular, the model performance, storage, and compression / decompression efficiency are benchmarked for CNNs. Empirical results based on information theory show that neighboring subtensors with implicit / latent information cannot be identified for data reconstruction. The robustness of tensor network representations subject to perturbation of the subtensors is also investigated.

- Propose a theory based on subspace analysis using singular value decomposition (SVD) for adversarial examples in CNNs. Using the theory, we quantify the robustness of different datasets to adversarial attacks, analyze the efficacy of different defense techniques based on input transformation and the structural similarity of different adversarial attacks. The theory is extended to analyze higher-order tensors with tensor-train SVD (TT-SVD) and an efficient algorithm is proposed to detect strong and static adversarial attacks (see Fig. 1).

The organization of this paper is as follows: Section 2 presents the preliminary knowledge of tensor networks such as tensor formats, properties, and storage complexity. The proposed robust TT-SVD algorithm for adversarial detection is presented in Section 2.1. Section 3 covers the threat model, adversarial attacks and defenses in CNNs. Experimental studies are conducted and the results are discussed in Section 4. Section 5 and 6 provide the related work and conclusion respectively.

2. Tensor Networks (TN)

Tensor decomposition has found many applications in signal processing and machine learning. Many review papers have been published throughout the years, more recent and relevant to machine learning and big data applications include [14, 16, 61, 56, 15, 5, 25]. The basic tensor formats and properties are summarized here.

Canonical Polyadic (CP) decomposition is one of the most popular tensor technique due to the ease of interpretation. CP is expressed as the sum of rank-1 components

$$A(i_1, \cdots, i_d) \cong \sum_{r=1}^{R} U_1(i_1, r) \, U_2(i_2, r) \cdots U_d(i_d, r), \quad (1)$$

where A is a d-dimensional tensor, r is the canonical rank and U_j is the latent factor in scalar representation. Each rank-one component of the decomposition serves as a latent concept or cluster in the data. The latent factors can be interpreted as soft membership to the r-th latent cluster. CP is unique up to scaling and permutation of the r components under very mild conditions, i.e., the components should be "sufficiently different" and their number not unreasonably large. Although CP format bypasses the curse of dimensionality, CP approximation may involve numerical instabilities for very high-order tensors because the problem is generally ill-posed due to intrinsic uncloseness.

Tucker decomposition (TD) captures the interactions between the latent factors U_i using a core tensor G that reflects the main subspace variation in each mode assuming a multilinear structure, TD is in the form of

$$A(i_1, \cdots, i_d) \cong \sum_{r_1=1}^{R_1} \sum_{r_2=1}^{R_2} \cdots \sum_{r_d=1}^{R_d} G(r_1, r_2, \cdots, r_d)$$
$$U_1(i_1, r_1) \, U_2(i_2, r_2) \cdots U_d(i_d, r_d) \quad (2)$$

TD is non-unique because the latent factors can be rotated without affecting the reconstruction error. TD yields a good low-rank approximation of a tensor, since the core tensor G is the best compression of the original tensor with respect to squared error. However, Tucker format is not practical for tensor order $d > 5$ because the number of entries of the core tensor scales exponentially with d.

Hierarchical Tucker (HT) decomposition [27, 24] approximates well high-order tensors ($d \gg 3$) without suffering from the curse of dimensionality. HT requires a priori

TN	Storage Complexity	Storage Bound
CP	$\sum_{k=1}^{d} I_k R$	$O(dIR)$
TD	$\sum_{k=1}^{d} I_k R_k + \prod_{k=1}^{d} R_k$	$O(dIR + R^d)$
HT	$\sum_{k=1}^{d} I_k R_k + \sum_{u,v,t} R_u R_v R_t$	$O(dIR + dR^3)$
TT	$\sum_{k=1}^{d} I_k R_{k-1} R_k$	$O(dIR^2)$

Table 1. Storage complexity of TN [14]. d is the tensor order, I_k and R_k are the size and rank of mode k respectively. The storage bound is calculated by letting $I = \max_k I_k$ and $R = \max_k R_k$ for all possible k in particular TN.

knowledge of a binary tree of matricizations of the tensor,

$$A(i_1, \cdots, i_d) \cong \sum_{r_{u_0}=1}^{R_{u_0}} \sum_{r_{v_0}=1}^{R_{v_0}} B_{(12\cdots d)}(r_{u_0}, r_{v_0})$$
$$f_{u_0}(i_{u_0}, r_{u_0}) f_{v_0}(i_{v_0}, r_{v_0})$$
$$f_t(i_t, r_t) \cong \sum_{r_u=1}^{R_u} \sum_{r_v=1}^{R_v} B_t(r_u, r_v, r_t) f_u(i_u, r_u) f_v(i_v, r_v)$$
$$(3)$$

where B_t are "transfer" core tensors (internal nodes), f_u and f_v are the corresponding left and right child nodes respectively. The leaf nodes contain the latent factors.

Tensor-Train (TT) decomposition [55, 54] decomposes a given tensor into a matrix, followed by a series of three-mode "transfer" core tensors, and finally ended by a matrix. Each one of the core tensors is "connected" with its neighboring core tensors through a common reduced mode or so-called TT-rank r_k with $r_0 = r_d = 1$. TT is given by

$$A(i_1, \cdots, i_d) \cong \sum_{r_1=1}^{R_1} \sum_{r_2=1}^{R_2} \cdots \sum_{r_{d-1}=1}^{R_{d-1}} G_1(r_0, i_1, r_1)$$
$$G_2(r_1, i_2, r_2) \cdots G_d(r_{d-1}, i_d, r_d)$$
$$(4)$$

CP and TD are globally-additive models, which means tensors are represented by a (global) sum over few separable (rank-1) elements; whereas TT format is locally-multiplicative type, variables only interact directly with few local neighbors (slightly-entangled systems) through the contracted product representations. Table 1 tabulates the storage complexity and storage bound of different TN. TT format exhibits both very good numerical properties and allows control of the approximation error within the decomposition algorithm. Fig. 2 shows the TT-SVD algorithm for TT decomposition and Section 2.1 explains the basics of SVD. Mathematical operations in TT format increase the TT-ranks, TT-rounding algorithm, which is mathematically similar to TT-SVD but in TT format, can efficiently reduce the TT-ranks to optimal.
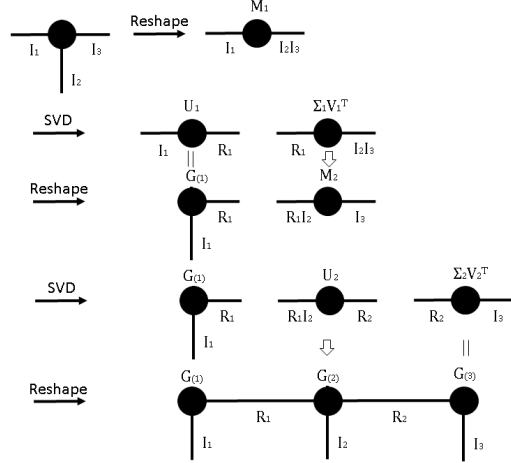

Figure 2. The TT-SVD algorithm for TT decomposition of a 3rd order tensor. M_k is the matricization of the subtensors. The ordering of indices I_k should be symmetric to get consistent SVD analyses (e.g. decay rate of singular values). For RGB color images, I_1: row indices, I_2: channels, and I_3: column indices. The decay rate is averaged over the sequences of SVD decomposition.

2.1. Robust TT-SVD Algorithm

Singular value decomposition (SVD) decomposes a matrix A into left and right singular vectors, the basis vectors are ranked by the amount of explained variation in A or the so-called singular values. Mathematically, SVD is given by $A \cong U\Sigma V^T$, where U and V are orthonormal matrices that contain the left and right singular vectors in their respective columns, the diagonal elements of Σ matrix contain the corresponding singular values. As shown in Fig. 3 and 4, the distribution of singular values affect the luminance variation that accounts for textural changes such as smoothness / roughness change; the singular vectors form the basis images that encode the structural information of the original image [51]. The TT-SVD algorithm in Fig. 2 is used to extend SVD analyses to higher-order tensors such as color images. Unlike discrete Fourier, cosine, or wavelet transform, the basis images of SVD are not fixed but adaptively-derived, thus allows better representation of the image structure. Perturbation theory of SVD shows that the closeness of a singular value from its neighbors controls the sensitivity of its singular vector to perturbations [63]. It is further shown that when two singular values are close enough, the corresponding singular vectors are not unique, approximation of the change in subspace spanned by the corresponding singular vectors cannot be done with first-order perturbation theory but requires higher-order terms [46]. The singular values of real-life images follow exponential decay distribution, therefore the decay rate provides a scale-independent measure of the closeness of singular values and allows comparison of the robustness of multiscale corre-

3

Figure 3. The effect of transferring singular values between images. Last image from top row shows the original image of a motorbike. Bottom row shows the change of luminance / texture after the transfer of singular value distribution from the top images. Last image on the bottom row shows the transfer of average of all the singular values of the top images.
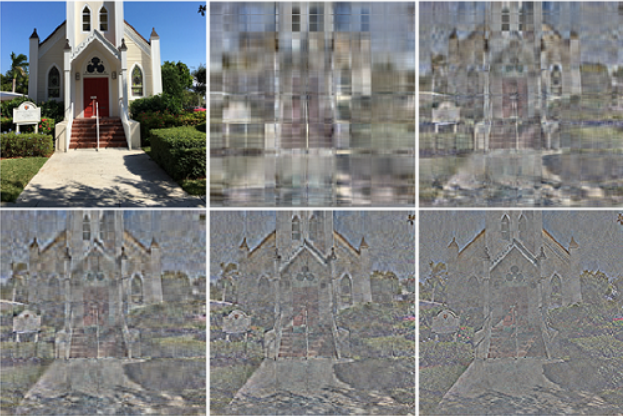
Figure 4. (Left to right, top to bottom) The original and reconstructed images by combining the left and right singular vectors from 10, 20, 30, 50, and 100 largest singular values. Singular vectors encode the multiscale correlation structure of the original image. It can be observed that large singular values are associated with large-scale variation (low frequency components) and vice versa for fine-scale variation (high frequency components).

lation structure to perturbations between different datasets and image-processing techniques.

Unlike SVD, the transform kernels of convolutional neural networks (CNN) are learned from data and fixed after the training is complete; the CNN filters are not constrained to be orthogonal, but the domain of possible filter choices for both SVD and CNN spans the input space. Once training is complete, the input subspace spanned by CNN's filters is a subset of the whole input space. To make it more precise, suppose we split the input into irrelevant and relevant parts $A + \Delta A$ that activate particular CNN's neuron, both parts share a subset of all the singular vectors, i.e., $A + \Delta A = U(\Sigma + \Delta\Sigma)V^T$. In the case that $||\Sigma|| >> ||\Delta\Sigma||$, the robustness of the subspace spanned by the corresponding singular vectors of $\Delta\Sigma$ is determined by the closeness of the set of singular values and their neighbors. There are a few loss terms in CNN: the approximation loss due to limited number of transform kernels, the rectification loss due to nonlinear activations, spatial pooling, and

dropout layers. The theoretical foundations of CNN in subspace approximation are laid down by Kuo [39, 40, 41, 12]. The research on subspace-based signal analysis using SVD is well-established among the signal processing community, in particular the sensitivity of subspace approximation with individual singular vectors when the singular values are close [69, 46]. If the singular values are well-separated, it can be shown that both the singular values and vectors change in the order of noise magnitude [64]. As will be shown in Section 4 Experiments, the decay rate of real-life images is small, therefore we hypothesize that the close separation between singular values gives rise to the adversarial examples in deep learning models, i.e., the neuron's activation patterns are not unique and extremely sensitive to input perturbations.

Additionally, we propose a robust SVD algorithm (Algorithm 1) to generate quasi-distinct singular values from closely-separated ones. In doing so, the resultant singular vectors are more robust to input perturbations, the reconstructed images are used to detect strong and static adversarial attacks. First, the cumulative sum in ascending order of the singular values, $\hat{S}$ is divided into multiple bins with exponentially-distributed bin edges. The singular values and corresponding singular vectors that fall within a bin are summed up and linearly-combined respectively. This is in accordance with the theory of degenerate matrix SVD such that any normalized linear combination of singular vectors that share the same singular value is a valid singular vector of that singular value. By merging with TT-SVD (see Fig. 2), the robust SVD algorithm can be extended to higher-order tensors such as 2D / 3D color images, videos, and hyperspectral images. The algorithm is efficient because the computational complexity increases linearly with the tensor mode size.

3. Adversarial Attacks and Defenses

Adversarial attacks can be targeted or untargeted; the choice / structure imposed on the input perturbations is typically shaped by an ℓ_p-norm distance metric and computed with gradient-based or optimization-based techniques with the objective to decrease the model performance. In our study, the adversarial strength is measured by normalized ℓ_2-dissimilarity [26], the adversary is assumed to know only the CNN models but has no ability to influence them.

Adversarial defenses can be broadly categorized into adversarial training and input transformations. Adversarial training requires prior knowledge of the type of attacks and train the models to differentiate them, therefore the amount of computational cost is much higher. Input transformations use either traditional image-processing techniques or generative models to remove adversarial examples; the technique is less expensive but susceptible to adaptive attacks who know the transformation techniques. We focus on in-

Algorithm 1 Robust SVD (can replace SVD in TT-SVD or TT-rounding algorithms, see Fig. 2 for TT-SVD)

> **input:** matrix A.
> **parameter:** α, β of exponential distribution.
> **output:** quasi-distinct singular values S and corresponding (linearly-combined) singular vectors U, V.
>
> Initialize $\hat{S}_{binEdges} \leftarrow [0, \alpha \exp(\beta z)], z \in \{0, 1, \cdots\}$
> **begin**
> $[U_0, S_0, V_0] \leftarrow svd(A)$
> $\hat{S}_0 \leftarrow cumsum(S_0, `reverse')$
> $index \leftarrow bucketize(\hat{S}_0, \hat{S}_{binEdges})$
> $S \leftarrow accumArray(S_0, index, `sum')$
> $U \leftarrow accumArray(U_0, index, `average')$
> $V \leftarrow accumArray(V_0, index, `average')$
>   Rearrange S, U, V in descending order of S
>   Normalize $U \leftarrow \frac{U}{||U||_2}, V \leftarrow \frac{V}{||V||_2}$
>   (Optional) SVD rank truncation
>   Return S, U, V
> **end**

put transformations that have been used against adversarial attacks in previous studies and explain the reason of their effectiveness based on our proposed theory.

4. Experiments

Datasets. MNIST [45] is a widely used dataset for digit classification that was introduced in 1998. It consists of 28×28 pixel grayscale images of handwritten digits. There are 10 classes (10 digits), $60,000$ training images, and $10,000$ testing images. Street View House Numbers (SVHN) [52] is an MNIST-like 32×32 pixel color images consists of $73,257$ training images and 26032 testing images for 10 classes (10 digits). They are taken from Google Street View images and usually corrupted by natural phenomena like severe blur, distortion, and illumination effects on top of wide style and font variations [52]. CIFAR-10 [33] is a dataset released in 2009 that consists of 32×32 pixel color images of 10 mutually exclusive classes with $50,000$ training images and $10,000$ test images. ImageNet [60] is used for large-scale evaluation, it was first introduced in 2010 and the dataset stabilized in 2012. ImageNet contains color images of at least 256×256 pixel with 1000 classes; only the validation set consists of $50,000$ images (50 per class) are used. Section 4.1 benchmarks the TN storage complexity, algorithmic efficiency, and model performance using these datasets. The privacy and security issues in image recognition are studied using 1000 development (color) images of 299×299 pixel released in NIPS 2017 Adversarial Attacks and Defenses Competition. This dataset is referred to as "ImageNet" [60] in Section 4.2, 4.3, and 4.4 due to their similar task difficulty.

Experimental Setup. To compute the TN decomposition in Section 4.1, Matlab 2017a and several toolboxes are used: Tensorlab 3.0 [71], htucker 1.2 [32], and TT-toolbox 2.2.2. The compression and decompression time are benchmarked using Intel(R) Xeon(R) CPU E5-1650 v4 @ 3.60GHz 3.60GHz. CP and TD are computed using Tensorlab "cpd_gevd" and "mlsvd" functions, HT using htucker "htensor.truncate_ltr" function, and TT using TT-toolbox "tt_tensor" function. These functions use generalized eigenvalue or SVD to speed up the decomposition. Adversarial defenses based on input transformation using color bit-depth reduction [75], cropping-rescaling, median, gaussian, and non-local means [9] filters are coded using Matlab functions and toolbox. Image quilting [21], total variance minimization (TVM) [59], and JPEG compression [20] are Python implementations by Guo *et al.* [26]. Adversarial attacks are generated using Tensorflow 1.4.0 [2, 1] and Cleverhans v2.1.0 [57]. The CNN model for MNIST, SVHN, and CIFAR-10 is an all convolutional net [62] taken from Cleverhans model zoo. The ImageNet classification is using Inception v3 [66]. Fast Gradient Method (FGM) [22], Basic Iteration Method (BIM) [42], and Deep Fool (DF) [50] are gradient-based attacks whereas Carlini-Wagner (CW) [10] and Elastic Net Method (EAD) [11] are optimization-based adversarial attacks. We follow closely the method proposed by Guo *et al.* [26] to generate adversarial examples with increasing adversarial strength. FGM and BIM are done by adjusting the hyperparameters; DF and CW perturbations are amplified to increase the normalized ℓ_2-dissimilarity after successful attacks. Universal Perturbations (UP) [49] and Adversarial Patch (AP) [8] are strong static attacks which can be image- and network-agnostic. Only the image-agnostic case is considered here. UP is generated using BIM in each iteration; whereas AP is taken from the implementations by Brown *et al.* [8]. Different from other adversarial techniques that manipulate pixels within ℓ_p distance which may sometimes produce noticeable artifacts, spatially transformed adversarial example (stAdv) [74] is a new approach that generates realistic adversarial examples with smooth image deformation; their code is made publicly available by Dumont *et al.* [19]. In our study, AP and stAdv are targeted attacks with "toaster" and randomized targets respectively, others are untargeted attacks. Because stAdv deforms images smoothly, which stands in contrast to our proposed theory that adversarial examples tend to increase the image roughness, we report the stAdv hyperparameter that regularizes the local distortion characterized by a flow field and adversarial loss used in our study, i.e., MNIST (10^{-2}), SVHN (10^{-3}), CIFAR-10 (10^{-3}), and ImageNet (10^{-6}). Notice that the regularization decreases with dataset complexity, this means that it is much harder to generate adversarial examples with smooth deformation for complex images.

5

TN	Time (ms)	Compression Ratio	Top-1 Accuracy
MNIST Dataset			0.993
CP	N/A	N/A	N/A
TD	0.6 / 0.3	0.390	0.988
HT	2.5 / 0.5	0.422	0.988
TT	0.39 / 0.07	0.439	0.990
SVHN Dataset			0.951
CP	7.9 / 0.14	0.327	0.945
TD	1.6 / 0.37	0.309	0.950
HT	2.8 / 0.56	0.342	0.950
TT	0.97 / 0.07	0.150	0.929
CIFAR-10 Dataset			0.858
CP	7.8 / 0.13	0.334	0.811
TD	1.6 / 0.39	0.309	0.8105
HT	2.9 / 0.58	0.342	0.809
TT	1.2 / 0.09	0.455	0.833
ImageNet Dataset			0.748
CP	214 / 2.2	0.460	0.535
TD	53.9 / 4.3	0.335	0.693
HT	53.8 / 3.2	0.372	0.703
TT	48.3 / 2.7	0.501	0.655

Table 2. Model performance using TN for input data compression. The time for compression / decompression per image is measured in milliseconds. CP decomposition is not available (N/A) for MNIST dataset because of algorithmic instability. This happens occasionally for other datasets, hence the original data and size are used instead for calculation of compression ratio.

4.1. Dimensionality Reduction of Input Data

Table 2 benchmarks the compression / decompression time for TN with different compression ratio. The time needed generally increases with TN size. CP decomposition is about $4\times$ longer than other TN decomposition. TN decompression time is generally much faster compared to compression time. After TN decomposition, the cores and latent factors are quantized to 8-bit depth. Some of the subtensors can be uniformly quantized but some requires non-uniform quantization using Lloyd's algorithm [47, 48] to reduce the image distortion, e.g., TD's core G in Eq. 2. It can be observed that TN generally retains the features for image classification by CNNs without the need to retrain the model; at least half of the storage size can be saved using TN for data compression.

4.2. Privacy-Preserving Distributed Data Storage and Communication

Fig. 5 shows the image distortion as a result of adding noise to randomly-selected TN subtensor, the effect is larger if the perturbations is applied on the singular vectors corresponding to the leading singular values, however this infor-
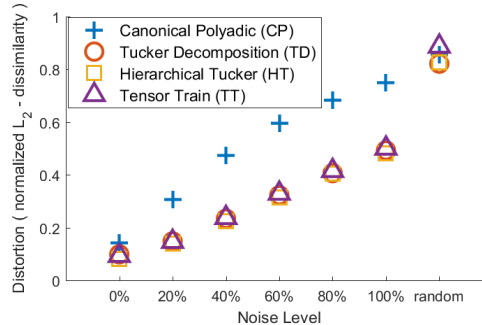

Figure 5. Image distortion resulted from adding noise to a randomly-selected core of the TN. Note that "random" label in the x-axis means randomize the sequence in the selected core.
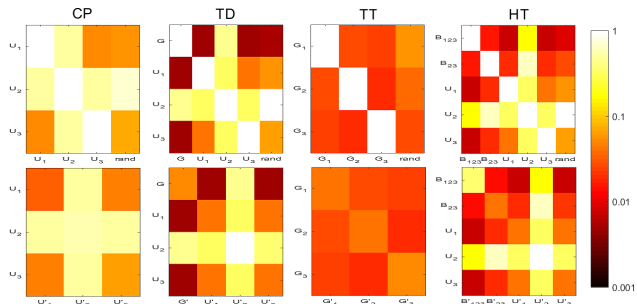

Figure 6. Normalized mutual information between cores and latent factors of one image (top row) and two different images (bottom row) for different TNs. Note that "rand" label in the x-axis means cores with uniformly-distributed noise.

mation is usually unknown to the adversary. CP's distortion is larger because the format is more compact compared to other TNs. Due to the diverse possible topology structure of decomposition for a given tensor, Wang *et al.* [72] proposes three different security models to process data generated by cyber-physical-social systems, i.e., open model, half-open model, and encrpted model to process data with different level of sensitivity and privacy requirements. The tensor formats and topology structure are made private to selected users for half-open and encrypted models. Here, we experimentally verify that the neighboring subtensors could not be identified based on information theory. Mutual information is commonly used to cross-examine the information content between subtensors [14]. Fig. 6 shows the normalized mutual information (NMI) between two subtensors of particular TN for one image, two images, and random noise, the results show that they are indistinguishable from each other. NMI is a universal metric such that any other distance measure judges two random variables close-by, NMI will also judge them close. As shown in Fig. 6. the NMI variation is largely attributed to the variation in subtensor's value distribution, if the variation in particular subtensor is high (i.e., entropy is high), its NMI with other subtensor is likely to be smaller.

Datasets	Image Size	TT-SVD Slope
MNIST (grayscale)	28x28x1	-0.4 ± 0.5
SVHN (color)	32x32x3	-0.38 ± 0.12
CIFAR10 (color)	32x32x3	-0.17 ± 0.04
ImageNet (color)	299x299x3	-0.072 ± 0.019
ImageNet (color) + 30% noise	299x299x3	-0.061 ± 0.016

Table 3. Robustness of correlation structure of different datasets measured by the TT-SVD slope. Steeper slope means the separation between singular values are larger, hence the subspace approximation by CNNs is more robust to input perturbations. The standard deviation of the TT-SVD slope measures the variability of the estimated value. Notice that adding noise flattens the TT-SVD slope, hence decreases the robustness of correlation structure.

4.3. Robustness against Adversarial Attacks

The decay rate of leading singular values determines the robustness of subspace approximation by CNNs. Table 3 tabulates the decay rate for 1000 randomly-selected images from MNIST, SVHN, CIFAR-10, and ImageNet datasets using the 5th-25th largest singular values. Coincidentally, the decay rate correlates well to the datasets' complexity. Fig. 7 shows the robustness of the datasets to adversarial attacks. It can be observed that the steeper the dataset's TT-SVD slope, the more robust the dataset to a wide variety of different adversarial attacks. In particular, input perturbations by stAdv is done by smooth deformation; it requires much higher adversarial strength for successful attacks compared to other techniques. This agrees with our theory that adversarial examples tend to decrease the decay rate of singular values to increase sensitivity of the subspace approximation by CNNs, hence increase the image roughness as a result. Table 4 shows that strong adversarial attacks flatten the TT-SVD slope. Effectiveness of defenses based on input transformation has been studied before, our theory explains the reason why spatial smoothing techniques provide more resistance to adversarial attacks, as shown in [26, 75]. This is because spatial smoothing steepen the TT-SVD slope (see Table 5), hence reduce the sensitivity of subspace approximation by CNNs.

4.4. Detect Strong and Static Adversarial Attacks

As shown in Table 6, the detection of strong static attacks using our proposed robust TT-SVD algorithm only requires bounding the ℓ_2-norm between image before and after reconstruction. Currently, the proposed algorithm works well if the image consists of "simple" correlation structure (high SVD's decay rate), e.g., single object recognition. Images with complex variation or cluttered scene may consider preprocessing with spatial smoothing and cropping-rescaling [23] respectively before using the proposed algorithm. Existing adversarial detection techniques rely on (1) sample
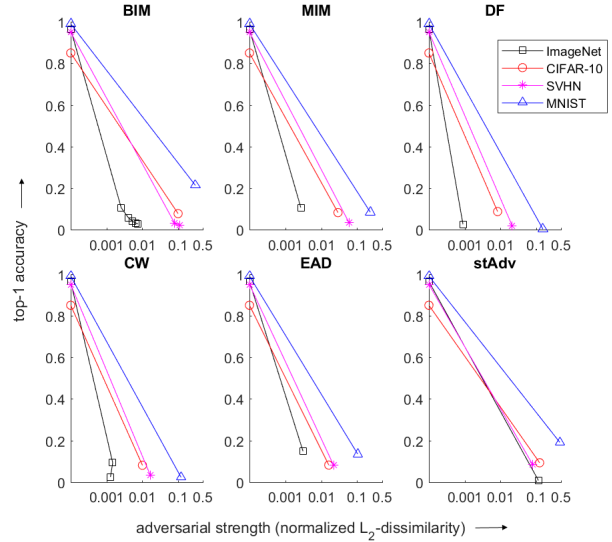

Figure 7. Model accuracy of datasets under adversarial attacks with increasing adversarial strength measured in normalized ℓ_2-dissimilarity. Notice the robustness of the datasets to adversarial attacks, i.e., MNIST > SVHN $\gtrsim$ CIFAR-10 > ImageNet.

Adversarial Attacks (Strength)	Top-1 Accuracy	TT-SVD Slope
FGM, ℓ_∞ (0.0812)	0.25	$-0.068 \pm 0.017 \uparrow$
FGM, ℓ_2 (0.0773)	0.25	$-0.067 \pm 0.016 \uparrow$
BIM, ℓ_∞ (0.0778)	0.016	$-0.069 \pm 0.017 \uparrow$
BIM, ℓ_2 (0.0784)	0.014	$-0.068 \pm 0.016 \uparrow$
CW, ℓ_2 (0.0775)	0.17	$-0.067 \pm 0.017 \uparrow$
DF, ℓ_2 (0.0765)	0.134	$-0.066 \pm 0.016 \uparrow$
UP, ℓ_∞ (0.0832)	0.196	$-0.068 \pm 0.017 \uparrow$
UP, ℓ_2 (0.0787)	0.196	$-0.068 \pm 0.017 \uparrow$
AP (0.64)	0.0	$-0.062 \pm 0.008 \uparrow$

Table 4. Similar to Table 3 but for adversarial attacks. Adversarial strength is measured by normalized ℓ_2-dissimilarity. The upwards arrow means that the technique flattens the TT-SVD slope by more than 10% of the slope variability, vice versa for downwards arrow. The original slope value is -0.072 ± 0.019.

statistics, (2) prediction inconsistency, and (3) training a detector; (1) is ineffective, (2) needs to process a batch of images each time, (3) needs to have labelled data and model training takes time [75]. The robust TT-SVD algorithm provides a new way to detect adversarial examples directly on the input; the algorithm is adaptive in nature because the singular values / vectors are adaptively-derived.

5. Related Work

Tensor decomposition has been used for feature extraction and classification on multidimensional data [58], recent work is extended to high-dimensional data with cutting-

Adversarial Defenses based on Input Transformation		TT-SVD Slope
Spatial Smoothing		
Cropping-Rescaling [23]		$-0.089 \pm 0.026 \downarrow$
Image Quilting [21]		$-0.079 \pm 0.019 \downarrow$
Median Filter [75]		$-0.080 \pm 0.020 \downarrow$
Gaussian Filter [75]		$-0.088 \pm 0.022 \downarrow$
Non-Local Means Filter [9]		$-0.081 \pm 0.021 \downarrow$
Total Variance Minimization [59]		$-0.081 \pm 0.020 \downarrow$
Amplitude Quantization		
Color Bit-Depth Reduction [75]	4-bit	-0.071 ± 0.018
	3-bit	$-0.069 \pm 0.017 \uparrow$
Frequency-based Compression		
JPEG [20] Compression	quality level	
	75	-0.072 ± 0.019
	50	-0.073 ± 0.019
	25	-0.073 ± 0.019
	5	-0.071 ± 0.017

Table 5. Similar to Table 4 but for adversarial defenses.

Adversarial Attacks	Norm	Adversarial Strength	Detection Rate
FGM [22]	ℓ_∞	0.071	0.997
	ℓ_2	0.043	0.956
BIM [42]	ℓ_∞	0.069	0.997
	ℓ_2	0.048	0.985
CW [10]	ℓ_2	0.046	0.944
DF [50]	ℓ_2	0.037	0.932
UP [49]	ℓ_∞	0.052	0.997
	ℓ_2	0.056	0.994
AP [8]	-	0.045	0.991

Table 6. Detection rate of strong and static adversarial attacks. The adversarial strength is measured by normalized ℓ_2-dissimilarity. The slope of cumulative distribution of TT-SVD is set to -0.03 and truncation error $\leqslant 0.03$. 337 out of 1000 development images from NIPS 2017 Adversarial Attacks and Defenses Competition are selected by setting the initial ℓ_2-norm < 1000. The ℓ_2-dissimilarity of the 337 samples is 0.01. Adversarial attacks are detected when ℓ_2-norm > 1000.

edge tensor techniques such as tensor-train decomposition [6, 7]. Theoretical links between tensor networks and deep learning are slowly establishing, for example, the expressive power of CP and HT decompositions correspond to shallow and deep networks respectively [17, 18], whereas TT corresponds to recurrent neural network [29]. Tensor networks have been used to compress and accelerate deep learning models due to the high redundancy in model parameters, e.g., fully-connected network [53], convolutional network [30, 67, 43], recurrent network [68], sharing residual units [79], multitask learning [77], multimodal

data [81, 82, 80, 13, 31]. Additionally, tensor power technique is used to learn latent variable models efficiently with statistically consistent estimator [5, 28]. Due to the versatility of tensor representations, tensor techniques have been proposed for big data networking and management [78, 37, 38, 76, 34], e.g., Internet of Things [3, 36]. Privacy-preserving techniques for tensor decomposition have also been studied [73, 35] for cloud computing. Exploring tensor networks as an alternative data structure for efficient and distributed storage as well as privacy preservation for input data of deep learning or other machine learning models have not be been considered before; our study is particularly relevant in the context of edge and fog computing. We exploit the data redundancy and uses tensor network decomposition to retain the relevant features for image classification.

In the field of computer vision, SVD has been used for image denoising, compression, and forensic such as steganography and watermarking. Higher-order SVD can help to disentangle the constituents factors or modes of image ensembles, e.g., TensorFaces [70] for facial images with different lighting conditions, viewpoint and poses. Closely related to our work is the use of SVD to extract features for visual quality assessment. Reference images are usually provided for comparison between images before and after processing [51], whereas no reference measure requires assumptions on the patches to be analyzed such as anisotropy [83]; all of the SVD-based image quality metrics work on grayscale images. Adversary does not provide the reference images for comparison; our work extends the SVD properties to higher-order tensors and analyze the robustness of correlation structure extracted from input data for image classification by CNNs.

6. Conclusion

At first glance, it may seems obvious that adversarial attacks increase the image roughness, therefore natural choices for adversarial defense based on input transformation should incorporate different levels of spatial smoothing, e.g., local, non-local, edge-preserving, etc. Further experiments show that the robustness against adversarial attacks differ between datasets with different decay rate of SVD singular values. This suggests that there is a deeper level connections between adversarial examples in deep learning models and SVD's decay rate. Perturbation theory of SVD shows that the closeness between singular values controls the sensitivity of subspace approximation by CNNs. Empirical results show that real-life images typically have slow SVD's decay rate, which explains the cause of adversarial examples in CNNs. The subspace approximation is more stable to input perturbations if the CNN's loss from approximation, pooling, dropout, and rectification can be reduced.

References

[1] M. Abadi, A. Agarwal, P. Barham, E. Brevdo, Z. Chen, C. Citro, G. S. Corrado, A. Davis, J. Dean, M. Devin, S. Ghemawat, I. Goodfellow, A. Harp, G. Irving, M. Isard, Y. Jia, R. Jozefowicz, L. Kaiser, M. Kudlur, J. Levenberg, D. Mané, R. Monga, S. Moore, D. Murray, C. Olah, M. Schuster, J. Shlens, B. Steiner, I. Sutskever, K. Talwar, P. Tucker, V. Vanhoucke, V. Vasudevan, F. Viégas, O. Vinyals, P. Warden, M. Wattenberg, M. Wicke, Y. Yu, and X. Zheng. TensorFlow: Large-scale machine learning on heterogeneous systems, 2015. Software available from tensorflow.org.

[2] M. Abadi, P. Barham, J. Chen, Z. Chen, A. Davis, J. Dean, M. Devin, S. Ghemawat, G. Irving, M. Isard, et al. Tensorflow: a system for large-scale machine learning. In *OSDI*, volume 16, pages 265–283, 2016.

[3] E. Acar, A. Anandkumar, L. Mullin, S. Rusitschka, and V. Tresp. Tensor computing for internet of things. *Dagstuhl Reports*, 6:57–79, 2016.

[4] N. Akhtar and A. Mian. Threat of adversarial attacks on deep learning in computer vision: A survey. *arXiv preprint arXiv:1801.00553*, 2018.

[5] A. Anandkumar, R. Ge, D. J. Hsu, S. M. Kakade, and M. Telgarsky. Tensor decompositions for learning latent variable models. *Journal of Machine Learning Research*, 15(1):2773–2832, 2014.

[6] J. A. Bengua, P. N. Ho, H. D. Tuan, and M. N. Do. Matrix product state for higher-order tensor compression and classification. *IEEE Transactions on Signal Processing*, 65(15):4019–4030, 2017.

[7] J. A. Bengua, H. N. Phien, and H. D. Tuan. Optimal feature extraction and classification of tensors via matrix product state decomposition. In *Big Data (BigData Congress), 2015 IEEE International Congress on*, pages 669–672. IEEE, 2015.

[8] T. B. Brown, D. Mané, A. Roy, M. Abadi, and J. Gilmer. Adversarial patch. *In Machine Learning and Computer Security Workshop, Neural Information Processing Systems*, 2017.

[9] A. Buades, B. Coll, and J.-M. Morel. A non-local algorithm for image denoising. In *Computer Vision and Pattern Recognition, 2005. CVPR 2005. IEEE Computer Society Conference on*, volume 2, pages 60–65. IEEE, 2005.

[10] N. Carlini and D. Wagner. Towards evaluating the robustness of neural networks. In *2017 IEEE Symposium on Security and Privacy (SP)*, pages 39–57. IEEE, 2017.

[11] P.-Y. Chen, Y. Sharma, H. Zhang, J. Yi, and C.-J. Hsieh. Ead: elastic-net attacks to deep neural networks via adversarial examples. *arXiv preprint arXiv:1709.04114*, 2017.

[12] Y. Chen, Z. Xu, S. Cai, Y. Lang, and C.-C. J. Kuo. A saak transform approach to efficient, scalable and robust handwritten digits recognition. In *2018 Picture Coding Symposium (PCS)*, pages 174–178. IEEE, 2018.

[13] J.-T. Chien and Y.-T. Bao. Tensor-factorized neural networks. *IEEE transactions on neural networks and learning systems*, 2017.

[14] A. Cichocki, N. Lee, I. Oseledets, A.-H. Phan, Q. Zhao, and D. P. Mandic. Tensor networks for dimensionality reduction and large-scale optimization: Part 1 low-rank tensor decompositions. *Foundations and Trends® in Machine Learning*, 9(4-5):249–429, 2016.

[15] A. Cichocki, D. Mandic, L. De Lathauwer, G. Zhou, Q. Zhao, C. Caiafa, and H. A. Phan. Tensor decompositions for signal processing applications: From two-way to multiway component analysis. *IEEE Signal Processing Magazine*, 32(2):145–163, 2015.

[16] A. Cichocki, A.-H. Phan, Q. Zhao, N. Lee, I. Oseledets, M. Sugiyama, and D. P. Mandic. Tensor networks for dimensionality reduction and large-scale optimization: Part 2 applications and future perspectives. *Foundations and Trends® in Machine Learning*, 9(6):431–673, 2017.

[17] N. Cohen, O. Sharir, and A. Shashua. On the expressive power of deep learning: A tensor analysis. In *Conference on Learning Theory*, pages 698–728, 2016.

[18] N. Cohen and A. Shashua. Convolutional rectifier networks as generalized tensor decompositions. In *International Conference on Machine Learning*, pages 955–963, 2016.

[19] B. Dumont, S. Maggio, and P. Montalvo. Robustness of rotation-equivariant networks to adversarial perturbations. *arXiv preprint arXiv:1802.06627*, 2018.

[20] G. K. Dziugaite, Z. Ghahramani, and D. M. Roy. A study of the effect of jpg compression on adversarial images. *arXiv preprint arXiv:1608.00853*, 2016.

[21] A. A. Efros and W. T. Freeman. Image quilting for texture synthesis and transfer. In *Proceedings of the 28th annual conference on Computer graphics and interactive techniques*, pages 341–346. ACM, 2001.

[22] I. Goodfellow, J. Shlens, and C. Szegedy. Explaining and harnessing adversarial examples. *In Proc. ICLR*, 2015.

[23] A. Graese, A. Rozsa, and T. E. Boult. Assessing threat of adversarial examples on deep neural networks. In *Machine Learning and Applications (ICMLA), 2016 15th IEEE International Conference on*, pages 69–74. IEEE, 2016.

[24] L. Grasedyck. Hierarchical singular value decomposition of tensors. *SIAM Journal on Matrix Analysis and Applications*, 31(4):2029–2054, 2010.

[25] L. Grasedyck, D. Kressner, and C. Tobler. A literature survey of low-rank tensor approximation techniques. *GAMM Mitteilungen*, 36(1):53–78, 2013.

[26] C. Guo, M. Rana, M. Cisse, and L. van der Maaten. Countering adversarial images using input transformations. *ICLR*, 2017.

[27] W. Hackbusch and S. Kühn. A new scheme for the tensor representation. *Journal of Fourier analysis and applications*, 15(5):706–722, 2009.

[28] M. Janzamin, H. Sedghi, and A. Anandkumar. Beating the perils of non-convexity: Guaranteed training of neural networks using tensor methods. *arXiv preprint arXiv:1506.08473*, 2015.

[29] V. Khrulkov, A. Novikov, and I. Oseledets. Expressive power of recurrent neural networks. *arXiv preprint arXiv:1711.00811*, 2017.

[30] Y.-D. Kim, E. Park, S. Yoo, T. Choi, L. Yang, and D. Shin. Compression of deep convolutional neural networks for fast and low power mobile applications. *ICLR*, 2015.

[31] J. Kossaifi, A. Khanna, Z. Lipton, T. Furlanello, and A. Anandkumar. Tensor contraction layers for parsimonious deep nets. In *Computer Vision and Pattern Recognition Workshops (CVPRW), 2017 IEEE Conference on*, pages 1940–1946. IEEE, 2017.

[32] D. Kressner and C. Tobler. htucker - a matlab toolbox for tensors in hierarchical tucker format. *Mathicse, EPF Lausanne*, 2012.

[33] A. Krizhevsky, V. Nair, and G. Hinton. Learning multiple layers of features from tiny images. 2009.

[34] L. Kuang, F. Hao, L. T. Yang, M. Lin, C. Luo, and G. Min. A tensor-based approach for big data representation and dimensionality reduction. *IEEE transactions on emerging topics in computing*, 2(3):280–291, 2014.

[35] L. Kuang, L. Yang, J. Feng, and M. Dong. Secure tensor decomposition using fully homomorphic encryption scheme. *IEEE Transactions on Cloud Computing*, 2015.

[36] L. Kuang, L. T. Yang, and K. Qiu. Tensor-based software-defined internet of things. *IEEE Wireless Communications*, 23(5):84–89, 2016.

[37] L. Kuang, L. T. Yang, S. C. Rho, Z. Yan, and K. Qiu. A tensor-based framework for software-defined cloud data center. *ACM Transactions on Multimedia Computing, Communications, and Applications (TOMM)*, 12(5s):74, 2016.

[38] L. Kuang, L. T. Yang, X. Wang, P. Wang, and Y. Zhao. A tensor-based big data model for qos improvement in software defined networks. *IEEE Network*, 30(1):30–35, 2016.

[39] C.-C. J. Kuo. The cnn as a guided multilayer recos transform [lecture notes]. *IEEE Signal Processing Magazine*, 34(3):81–89, 2017.

[40] C.-C. J. Kuo and Y. Chen. On data-driven saak transform. *Journal of Visual Communication and Image Representation*, 50:237–246, 2018.

[41] C.-C. J. Kuo, M. Zhang, S. Li, J. Duan, and Y. Chen. Interpretable convolutional neural networks via feedforward design. *arXiv preprint arXiv:1810.02786*, 2018.

[42] A. Kurakin, I. Goodfellow, and S. Bengio. Adversarial examples in the physical world. *arXiv preprint arXiv:1607.02533*, 2016.

[43] V. Lebedev, Y. Ganin, M. Rakhuba, I. Oseledets, and V. Lempitsky. Speeding-up convolutional neural networks using fine-tuned cp-decomposition. *ICLR*, 2015.

[44] Y. LeCun, Y. Bengio, and G. Hinton. Deep learning. *Nature*, 521(7553):436–444, 2015.

[45] Y. LeCun, C. Cortes, and C. J. Burges. The mnist database of handwritten digits. 1998.

[46] J. Liu, X. Liu, and X. Ma. First-order perturbation analysis of singular vectors in singular value decomposition. *IEEE Transactions on Signal Processing*, 56(7):3044–3049, 2008.

[47] S. Lloyd. Least squares quantization in pcm. *IEEE transactions on information theory*, 28(2):129–137, 1982.

[48] J. Max. Quantizing for minimum distortion. *IRE Transactions on Information Theory*, 6(1):7–12, 1960.

[49] S.-M. Moosavi-Dezfooli, A. Fawzi, O. Fawzi, and P. Frossard. Universal adversarial perturbations. In *Proceedings of the IEEE Conference on Computer Vision and Pattern Recognition*, pages 1765–1773, 2017.

[50] S.-M. Moosavi-Dezfooli, A. Fawzi, and P. Frossard. Deepfool: a simple and accurate method to fool deep neural networks. In *Proceedings of the IEEE Conference on Computer Vision and Pattern Recognition*, pages 2574–2582, 2016.

[51] M. Narwaria and W. Lin. Svd-based quality metric for image and video using machine learning. *IEEE Transactions on Systems, Man, and Cybernetics, Part B (Cybernetics)*, 42(2):347–364, 2012.

[52] Y. Netzer, T. Wang, A. Coates, A. Bissacco, B. Wu, and A. Y. Ng. Reading digits in natural images with unsupervised feature learning. In *NIPS workshop on deep learning and unsupervised feature learning*, volume 2011, page 5, 2011.

[53] A. Novikov, D. Podoprikhin, A. Osokin, and D. P. Vetrov. Tensorizing neural networks. In *Advances in Neural Information Processing Systems 28*, pages 442–450. 2015.

[54] I. Oseledets and E. Tyrtyshnikov. Tt-cross approximation for multidimensional arrays. *Linear Algebra and its Applications*, 432(1):70–88, 2010.

[55] I. V. Oseledets. Tensor-train decomposition. *SIAM Journal on Scientific Computing*, 33(5):2295–2317, 2011.

[56] E. E. Papalexakis, C. Faloutsos, and N. D. Sidiropoulos. Tensors for Data Mining and Data Fusion. *ACM Transactions on Intelligent Systems and Technology*, 8(2):1–44, 2016.

[57] N. Papernot, P. McDaniel, A. Sinha, and M. Wellman. Towards the science of security and privacy in machine learning. *arXiv preprint arXiv:1611.03814*, 2016.

[58] A. H. Phan and A. Cichocki. Tensor decompositions for feature extraction and classification of high dimensional datasets. *Nonlinear theory and its applications, IEICE*, 1(1):37–68, 2010.

[59] L. I. Rudin, S. Osher, and E. Fatemi. Nonlinear total variation based noise removal algorithms. *Physica D: nonlinear phenomena*, 60(1-4):259–268, 1992.

[60] O. Russakovsky, J. Deng, H. Su, J. Krause, S. Satheesh, S. Ma, Z. Huang, A. Karpathy, A. Khosla, M. Bernstein, et al. Imagenet large scale visual recognition challenge. *International Journal of Computer Vision*, 115(3):211–252, 2015.

[61] N. D. Sidiropoulos, L. D. Lathauwer, X. Fu, K. Huang, E. E. Papalexakis, and C. Faloutsos. Tensor decomposition for signal processing and machine learning. *IEEE Transactions on Signal Processing*, 65(13):3551–3582, July 2017.

[62] J. T. Springenberg, A. Dosovitskiy, T. Brox, and M. Riedmiller. Striving for simplicity: The all convolutional net. *arXiv preprint arXiv:1412.6806*, 2014.

[63] G. W. Stewart. Stochastic perturbation theory. *SIAM review*, 32(4):579–610, 1990.

[64] G. W. Stewart. Perturbation theory for the singular value decomposition. *In SVD and Signal Processing, II: Algorithms, Analysis and Applications*, 1991.

[65] V. Sze, Y.-H. Chen, T.-J. Yang, and J. S. Emer. Efficient processing of deep neural networks: A tutorial and survey. *Proceedings of the IEEE*, 105(12):2295–2329, 2017.

[66] C. Szegedy, V. Vanhoucke, S. Ioffe, J. Shlens, and Z. Wojna. Rethinking the inception architecture for computer vision. In *Proceedings of the IEEE conference on computer vision and pattern recognition*, pages 2818–2826, 2016.

[67] C. Tai, T. Xiao, Y. Zhang, X. Wang, et al. Convolutional neural networks with low-rank regularization. *International Conference on Learning Representations*, 2015.

[68] A. Tjandra, S. Sakti, and S. Nakamura. Compressing recurrent neural network with tensor train. In *Neural Networks (IJCNN), 2017 International Joint Conference on*, pages 4451–4458. IEEE, 2017.

[69] A.-J. Van Der Veen, E. F. Deprettere, and A. L. Swindlehurst. Subspace-based signal analysis using singular value decomposition. *Proceedings of the IEEE*, 81(9):1277–1308, 1993.

[70] M. A. O. Vasilescu and D. Terzopoulos. Multilinear analysis of image ensembles: Tensorfaces. In *European Conference on Computer Vision*, pages 447–460. Springer, 2002.

[71] N. Vervliet, O. Debals, and L. De Lathauwer. Tensorlab 3.0 - numerical optimization strategies for large-scale constrained and coupled matrix/tensor factorization. In *Signals, Systems and Computers, 2016 50th Asilomar Conference on*, pages 1733–1738. IEEE, 2016.

[72] X. Wang, L. T. Yang, H. Liu, and M. J. Deen. A big data-as-a-service framework: State-of-the-art and perspectives. *IEEE Transactions on Big Data*, 4(3):325–340, 2018.

[73] Y. Wang and A. Anandkumar. Online and differentially-private tensor decomposition. In *Advances in Neural Information Processing Systems*, pages 3531–3539, 2016.

[74] C. Xiao, J.-Y. Zhu, B. Li, W. He, M. Liu, and D. Song. Spatially transformed adversarial examples. *ICLR*, 2018.

[75] W. Xu, D. Evans, and Y. Qi. Feature squeezing: Detecting adversarial examples in deep neural networks. *In The Network and Distributed System Security Symposium (NDSS)*, 2017.

[76] L. T. Yang, L. Kuang, J. Chen, F. Hao, and C. Luo. A holistic approach to distributed dimensionality reduction of big data. *IEEE Transactions on Cloud Computing*, 2015.

[77] Y. Yang and T. Hospedales. Deep multi-task representation learning: A tensor factorisation approach. *ICLR*, 2016.

[78] S. Yu, M. Liu, W. Dou, X. Liu, and S. Zhou. Networking for big data: A survey. *IEEE Communications Surveys & Tutorials*, 19(1):531–549, 2017.

[79] C. Yunpeng, J. Xiaojie, K. Bingyi, F. Jiashi, and Y. Shuicheng. Sharing residual units through collective tensor factorization in deep neural networks. *IJCAI*, 2017.

[80] Q. Zhang, L. T. Yang, Z. Chen, and P. Li. An improved deep computation model based on canonical polyadic decomposition. *IEEE Transactions on Systems, Man, and Cybernetics: Systems*, 2017.

[81] Q. Zhang, L. T. Yang, Z. Chen, and P. Li. A tensor-train deep computation model for industry informatics big data feature learning. *IEEE Transactions on Industrial Informatics*, 2018.

[82] Q. Zhang, L. T. Yang, X. Liu, Z. Chen, and P. Li. A tucker deep computation model for mobile multimedia feature learning. *ACM Transactions on Multimedia Computing, Communications, and Applications (TOMM)*, 13(3s):39, 2017.

[83] X. Zhu and P. Milanfar. Automatic parameter selection for denoising algorithms using a no-reference measure of image content. *IEEE transactions on image processing*, 19(12):3116–3132, 2010.